Model-based linear–quadratic–integral controller for simultaneous regulation of the current profile and normalized beta in NSTX-U

Hassan Al Khawaldeh *, Brian Leard, Sai Tej Paruchuri, Tariq Rafiq, Eugenio Schuster

Department of Mechanical Engineering and Mechanics, Lehigh University, Bethlehem, PA 18015, United States of America

ARTICLE INFO

ABSTRACT

Achieving advanced scenarios that are characterized by steady-state operation, stable plasma confinement, and high-performance plasmas is one of the primary objectives of the National Spherical Tokamak eXperiment-Upgrade (NSTX-U). Active control of the plasma may be necessary to achieve these conditions. In particular, control algorithms that can simultaneously optimize the shapes and values of plasma profiles and scalars, respectively, may play a critical role in robustly achieving and sustaining these advanced scenarios. In this work, a model-based optimal control algorithm is developed for feedback control of the current profile in NSTX-U. The linear, finite-dimensional, control model is derived by discretizing and linearizing the magnetic diffusion equation in combination with empirical correlations for electron density, electron temperature, and noninductive current drives. The linear, time-variant model is then used for designing a linear–quadratic–integral (LQI) controller that is capable of regulating both the safety factor and the normalized beta around desired targets. The controller determines the neutral beam injection powers and the overall plasma current that are needed to achieve the desired current profile and normalized beta. The proposed controller is tested in higher-fidelity nonlinear simulations that employ 1D models for the evolutions of both current and temperature profiles using the Control Oriented Transport SIMulator (COTSIM). The closed-loop simulations show the effectiveness of the controller at shaping the safety factor in NSTX-U while achieving the desired normalized beta.

1. Introduction

The National Spherical Tokamak eXperiment-Upgrade (NSTX-U) is one of the major spherical torus facilities in the world. NSTX-U went through two primary upgrades that differentiates it from the former NSTX device. The first upgrade is a complete replacement of the center stack, the Ohmic heating, and some divertor coils. Due to these replacements, both the toroidal field and the plasma current capabilities have increased from 0.55 to 1.0 T and 1.3 to 2.0 MA, respectively. The second upgrade is the addition of a second neutral beam injector with more tangential injection, which results in higher auxiliary heating power and neutral beam current drive. One of the NSTX-U objectives is to explore the capability of the spherical facility to produce and sustain advanced tokamak (AT) scenarios, which are characterized by steady-state operation, stable plasma confinement, and high-performance plasma [1].

The safety factor profile (a measure of the pitch of the helical magnetic field) and normalized beta (the ratio between kinetic and magnetic pressures) are plasma parameters critical to both the magnetohydrodynamic (MHD) stability and the performance of the confined plasma [2,3]. Thus, regulating these parameters simultaneously around the desired targets is essential to achieving AT scenarios. However, varying plasma conditions and external disturbances may make sustaining the desired scenario very difficult. Active control, i.e., feedforward + feedback control, could prove useful in regulating these plasma parameters around the desired targets in such cases.

Various feedback control algorithms have been proposed to control the safety-factor properties. Some of the existing control solutions across different tokamaks include robust control [4–6], nonlinear control [7–9], optimal control [10,11], and model predictive control [12–14]. Simultaneous control of the safety factor and the normalized beta has also been explored for machines such as EAST [15–17], DIII-D [18,19], and ITER [20]. An algorithm for simultaneous control of the central safety factor and normalized beta has been proposed for NSTX-U in [21]. However, a controller for simultaneous regulation of the whole safety factor profile and normalized beta for NSTX-U still needs to be developed.

In this work, a Linear–Quadratic–Integral (LQI) control algorithm is proposed to achieve such control objective. The proposed controller

---

* Corresponding author.
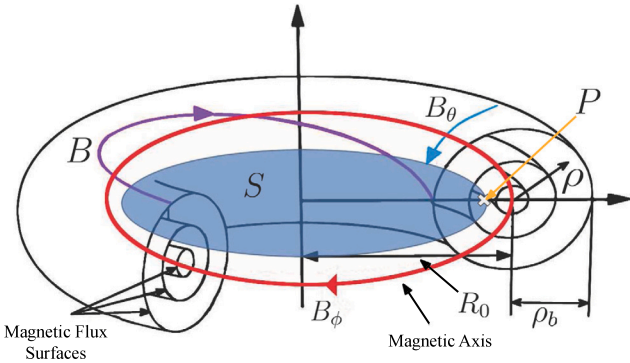 *E-mail address:* alkhawaldeh@lehigh.edu (H. Al Khawaldeh).

Fig. 1. Magnetic configuration in a tokamak.

augments and improves the previous LQI design presented in [11] in several ways. Firstly, the proposed controller is designed to regulate not only the safety factor profile but also the normalized beta. Secondly, the proposed controller determines in a direct way both the Neutral Beam Injection (NBI) powers and the plasma current to track the given targets. This is different from the LQI controller in [11], which determines the virtual inputs to achieve the control objective. The virtual inputs are then converted to actual inputs (NBI powers, plasma current, and line-averaged electron density) through solving an optimization problem in real time. The controller proposed in this work skips this step since it is synthesized using a linear model that treats the NBI powers and plasma current as the system inputs. Thirdly, the proposed controller regulates the safety factor profile and the normalized beta directly as opposed to the one proposed in [11], which regulates the safety factor profile indirectly through controlling the poloidal magnetic gradient. Finally, the proposed controller is tested in higher-fidelity nonlinear simulations that employ 1D models to predict the evolutions of both current and temperature profiles using the Control Oriented Transport SIMulator (COTSIM).

This paper is organized as follows. In Section 2, the control-oriented response models are introduced. In Section 3, both the model-reduction procedure and the control-algorithm design are thoroughly explained. In Section 4, simulation results for various objectives are presented. In Section 5, conclusions and future work are stated.

2. Models for poloidal magnetic flux and total energy

The helical magnetic field confining the plasma inside the tokamak is a combination of the toroidal magnetic field $\bar{B}_\phi$ and the poloidal magnetic field $\bar{B}_\theta$. Magnetic field lines around the torus map regions with identical poloidal magnetic flux Ψ. The poloidal magnetic flux at a point P is defined as $\Psi \triangleq \int_S \bar{B}_\theta \cdot d\bar{S}$, where $\bar{S}$ is the surface bounded by a toroidal ring that crosses a point P on the poloidal plane and is normal to the Z axis (Fig. 1). Under ideal MHD conditions, points with constant magnetic flux form nested surfaces [22]. Any variable that indexes the flux surfaces can be used as the spatial coordinate for spatially dependent plasma parameters like the safety factor profile. The chosen spatial coordinate in this work is the mean effective minor radius, which is defined as $\rho \triangleq \sqrt{\Phi/(B_{\phi,0}\pi)}$, where $B_{\phi,0}$ is the vacuum toroidal magnetic field at the magnetic axis, R_0 is the major radius, and Φ is the toroidal magnetic flux. The normalized mean effective minor is defined as $\hat{\rho} \triangleq \rho/\rho_b$, where ρ_b is the mean effective minor radius of the last closed flux surface.

The safety factor profile is defined as the ratio between the number of times a magnetic field line goes toroidally around the tokamak to the number of times it goes around poloidally,

$$q(\hat{\rho}, t) \triangleq \frac{d\Phi}{d\Psi} = -\frac{B_{\phi,0}\rho_b^2 \hat{\rho}}{\theta(\hat{\rho}, t)}, \tag{1}$$

$$\theta(\hat{\rho}, t) \triangleq \frac{\partial \psi}{\partial \hat{\rho}}, \tag{2}$$

$$\psi \triangleq \Psi/(2\pi), \tag{3}$$

where ψ is the poloidal stream function, and θ is the poloidal flux gradient.

2.1. Poloidal magnetic flux gradient profile

The evolution of the poloidal stream function ψ is given by the magnetic diffusion equation (MDE) [2,23]

$$\frac{\partial \psi}{\partial t} = \frac{\eta(T_e)}{\mu_0 \rho_b^2 \hat{F}^2} \frac{1}{\hat{\rho}} \frac{\partial}{\partial \hat{\rho}} \left[\hat{\rho} D_\psi(\hat{\rho}) \frac{\partial \psi}{\partial \hat{\rho}} \right] + R_0 \hat{H} \eta(T_e) \frac{\langle \bar{j}_{ni} \cdot \bar{B} \rangle}{B_{\phi,0}}, \tag{4}$$

subject to the boundary conditions

$$\frac{\partial \psi}{\partial \hat{\rho}}\Big|_{\hat{\rho}=0} = 0, \qquad \frac{\partial \psi}{\partial \hat{\rho}}\Big|_{\hat{\rho}=1} = -\frac{\mu_0 R_0}{2\hat{G}\hat{H}} I_p, \tag{5}$$

where η is the plasma resistivity, T_e is the electron temperature, μ_0 is the vacuum permeability, R_0 is the major radius, $\bar{j}_{ni}$ is the noninductive current density, $\bar{B}$ is the magnetic field, I_p is the total plasma current, $\langle . \rangle$ donates a flux-surface average, $D_\psi(\hat{\rho}) \triangleq \hat{F}(\hat{\rho})\hat{G}(\hat{\rho})\hat{H}(\hat{\rho})$ and

$$\hat{F} \triangleq \frac{R_0 B_{\phi,0}}{R B_\phi(R,Z)}, \quad \hat{G} \triangleq \langle \frac{R_0^2}{R^2} \mid \nabla \rho \mid^2 \rangle, \quad \hat{H} \triangleq \frac{\hat{F}}{\langle R_0^2/R^2 \rangle}. \tag{6}$$

To convert the MDE (4) into a model useful for control synthesis, control-oriented models for electron temperature, electron density, plasma resistivity, NBI current-drive, and bootstrap current-drive have been used in this work. A tight coupling between the electron and ion is assumed in this work although this assumption can easily be relaxed. Thus, the electron and ion densities and temperatures are assumed to be identical such as $n_e \approx n_i$ and $T_e \approx T_i$. The electron density is modeled as

$$n_e(\hat{\rho}, t) = n_e^{prof}(\hat{\rho})\bar{n}_e(t), \tag{7}$$

where n_e^{prof} is a normalized, nondimensional, reference electron-density profile, and $\bar{n}_e$ is the line-averaged electron density. The electron temperature profile is modeled as

$$T_e(\hat{\rho}, t) = k_{T_e}(\hat{\rho}) \frac{T_e^{prof}(\hat{\rho})}{n_e(\hat{\rho}, t)} I_p(t) \sqrt{P_{tot}(t)}, \tag{8}$$

where P_{tot} is the total power injected into the plasma, T_e^{prof} is a reference electron-temperature profile, I_p is the total plasma current, and k_{T_e} is a temperature profile constant. The resistivity is represented as

$$\eta(\hat{\rho}, t) = \frac{k_{sp}(\hat{\rho}) Z_{eff}}{T_e(\hat{\rho}, t)^{3/2}}, \tag{9}$$

where Z_{eff} is the effective atomic number, and k_{sp} is a constant profile. The noninductive current drive is produced by a combination of auxiliary neutral beam drive and the bootstrap current drive, and is expressed as

$$\frac{\langle \bar{j}_{ni} \cdot \bar{B} \rangle}{B_{\phi,0}}(\hat{\rho}, t) = \sum_{i=1}^{n_{nbi}} \frac{\langle \bar{j}_{nbi} \cdot \bar{B} \rangle}{B_{\phi,0}} + \frac{\langle \bar{j}_{bs} \cdot \bar{B} \rangle}{B_{\phi,0}}, \tag{10}$$

where $\bar{j}_{nbi}$ is the noninductive current generated by the NBIs, n_{nbi} is the number of NBIs, and $\bar{j}_{bs}$ is the noninductive current generated by bootstrap effect. The noninductive current drive generated by the ith NBI power is modeled as

$$\frac{\langle \bar{j}_{nbi} \cdot \bar{B} \rangle}{B_{\phi,0}} = k_{nbi}(\hat{\rho}) j_{nbi}^{dep}(\hat{\rho}) \frac{\sqrt{T_e(\hat{\rho}, t)}}{n_e(\hat{\rho}, t)} P_i(t), \tag{11}$$

where $i = 1, 2, \ldots, n_{nbi}$, P_i is the NBI power, k_{nbi} is a normalizing profile, and j_{nbi}^{dep} is a reference profile for each current-drive source, which are shown in Fig. 2.
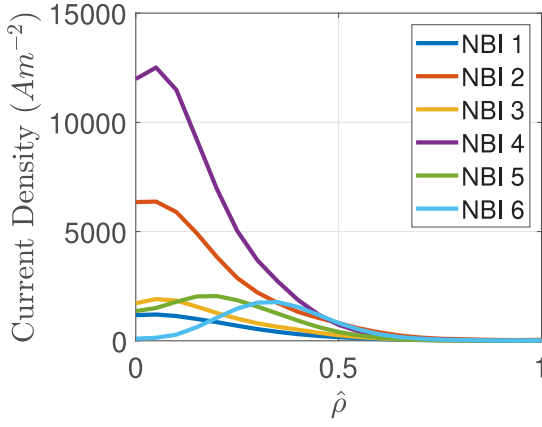
Fig. 2. Current deposition profile of NBIs.

The bootstrap current-drive is modeled as [24]

$$\frac{\langle \bar{j}_{bs} \cdot \bar{B} \rangle}{B_{\phi,0}} = \frac{R_0}{\hat{F}} \left[\frac{\partial \psi}{\partial \hat{\rho}} \right]^{-1} \times$$

$$(2\mathcal{L}_{31} T_e \frac{\partial n_e}{\partial \hat{\rho}} + \{2\mathcal{L}_{31} + \mathcal{L}_{32} + \alpha \mathcal{L}_{34}\} n_e \frac{\partial T_e}{\partial \hat{\rho}}), \qquad (12)$$

where $\mathcal{L}_{31}$, $\mathcal{L}_{32}$, $\mathcal{L}_{34}$, and α are factors that depend on the plasma magnetic configuration. Note that (12) assumes a tight coupling between electrons and ions as indicated before.

Substituting (7),(8),(9),(10) into (4) yields a model that is exploited in this work to design an LQI controller and has the form

$$\frac{\partial \psi}{\partial t} = f_\eta(\hat{\rho}) \frac{\bar{n}_e^{3/2}}{I_p^{3/2} P_{tot}^{3/4}} \frac{1}{\hat{\rho}} \frac{\partial}{\partial \hat{\rho}} \left[\hat{\rho} D_\psi(\hat{\rho}) \frac{\partial \psi}{\partial \hat{\rho}} \right]$$

$$+ \sum_{i=1}^{6} \left[f_i(\hat{\rho}) \frac{P_i}{I_p P_{tot}^{1/2}} \right] + f_{bs}(\hat{\rho}) \frac{\bar{n}_e^{3/2}}{I_p^{1/2} P_{tot}^{1/4}} \left[\frac{\partial \psi}{\partial \hat{\rho}} \right]^{-1}, \qquad (13)$$

where f_η, f_i, f_{bs} can be expressed in terms of the various model profiles and constants such as

$$f_\eta(\hat{\rho}) = \frac{k_{sp}(\hat{\rho}) Z_{eff} n_e^{prof}(\hat{\rho})^{3/2}}{\mu_0 \rho_b^2 \hat{F}(\hat{\rho}) k_{Te}(\hat{\rho})^{3/2} T_e^{prof}(\hat{\rho})^{3/2}}, \qquad (14)$$

$$f_i(\hat{\rho}) = R_0 \hat{H}(\hat{\rho}) k_{nbi}^{prof}(\hat{\rho}) j_{nbi}^{dep}(\hat{\rho}) \frac{k_{Te}(\hat{\rho})^{1/2} T_e^{prof}(\hat{\rho})^{1/2}}{n_e^{prof}(\hat{\rho})^{3/2}}, \qquad (15)$$

$$f_{bs}(\hat{\rho}) = \frac{k_{JeV} R_0^2 \hat{H}(\hat{\rho})}{\hat{F}(\hat{\rho})} \left[2\mathcal{L}_{31} \frac{dn_e^{prof}(\hat{\rho})}{d\hat{\rho}} \frac{k_{sp}(\hat{\rho}) Z_{eff} n_e^{prof}(\hat{\rho})^{1/2}}{k_{Te}(\hat{\rho})^{1/2} T_e^{prof}(\hat{\rho})^{1/2}} \right.$$

$$+ \{2\mathcal{L}_{31} + \mathcal{L}_{32} + \alpha \mathcal{L}_{34}\} \frac{d}{d\hat{\rho}} \left\{ \frac{k_{Te}(\hat{\rho}) T_e^{prof}(\hat{\rho})}{n_e^{prof}(\hat{\rho})} \right\}$$

$$\left. \frac{k_{sp}(\hat{\rho}) Z_{eff} n_e^{prof}(\hat{\rho})^{5/2}}{k_{Te}(\hat{\rho})^{3/2} T_e^{prof}(\hat{\rho})^{3/2}} \right]. \qquad (16)$$

In the following analysis, the spatial and time dependencies are dropped from all equations to simplify the presentation. Differentiating (13) on both sides with respect to the spatial variables $\hat{\rho}$ results in a partial differential equation (PDE) of the form

$$\frac{\partial \theta}{\partial t} = h_0 \frac{\bar{n}_e^{3/2}}{I_p^{3/2} P_{tot}^{3/4}} \theta'' + h_1 \frac{\bar{n}_e^{3/2}}{I_p^{3/2} P_{tot}^{3/4}} \theta' + h_2 \frac{\bar{n}_e^{3/2}}{I_p^{3/2} P_{tot}^{3/4}} \theta$$

$$+ f_{bs}' \frac{1}{\theta} \frac{\bar{n}_e^{3/2}}{I_p^{1/2} P_{tot}^{1/4}} + \sum_{i=1}^{6} f_i' \frac{P_i}{I_p P_{tot}^{1/2}}, \qquad (17)$$

subject to the boundary conditions

$$\theta \Big|_{\hat{\rho}=0} = 0, \qquad \theta \Big|_{\hat{\rho}=1} = -\frac{\mu_0 R_0}{2\hat{G}\hat{H}} I_p, \qquad (18)$$

where $(.)' = \partial/\partial \hat{\rho}$, and

$$h_0 = D_\psi f_\eta, \qquad (19)$$

$$h_1 = (2D_\psi' + \frac{1}{\hat{\rho}} D_\psi) f_\eta + D_\psi f_\eta', \qquad (20)$$

$$h_2 = (D_\psi'' + \frac{1}{\hat{\rho}} D_\psi' - \frac{1}{\hat{\rho}^2} D_\psi) f_\eta + (D_\psi' + \frac{1}{\hat{\rho}} D_\psi) f_\eta'. \qquad (21)$$

2.2. Plasma stored energy

The evolution of the plasma total energy W can be modeled as

$$\frac{dW(t)}{dt} = -\frac{W(t)}{\tau_E(t)} + P_{tot}(t). \qquad (22)$$

The energy confinement time τ_E is calculated using the IPB98(y,2) scaling law and represented as [25]

$$\tau_E = 0.0562 H_H I_p^{0.93} B_T^{0.15} R_0^{1.97} M^{0.19} \epsilon^{0.58} \bar{n}_{e,19}^{0.41} \kappa^{0.78} P_{tot}^{-0.69}, \qquad (23)$$

where H_H is the so-called H-factor, M is the plasma effective mass in amu, $\epsilon \triangleq a/R_0$ is the inverse aspect ratio, $\bar{n}_{e,19}$ is the line-average electron density in 10^{19} m^{-3}, and κ is the plasma elongation at the 95% flux surface.

The plasma stored energy W is related to the normalized beta β_N as follows

$$\beta_N = \frac{(2/3)W/V_p}{B_{\phi,0}^2/(2\mu_0)} \frac{a B_{\phi,0}}{I_p}, \qquad (24)$$

where V_p is the plasma volume, and a is the minor radius of the plasma.

3. Model reduction and control synthesis

3.1. Model reduction

A reduced-order model is needed for the synthesis of the feedback controller. The PDE described in (17) is discretized in space using a Taylor series approach. The infinite-dimensional model is discretized into n nodes using a uniform grid,

$$\Delta \hat{\rho} = \frac{1}{n-1}, \qquad \hat{\rho}_i = (i-1)\Delta \hat{\rho}, \qquad i = (1, \dots, n). \qquad (25)$$

Denoting θ at $\hat{\rho}_i$ as $\theta_i = \theta(\hat{\rho}_i, t)$, first-order Taylor series expansions are used to approximate the spatial derivatives of θ for the interior nodes $(2 \leq i \leq n-1)$, which take the form

$$\frac{\partial \theta}{\partial \hat{\rho}} \Big|_{\hat{\rho}=\hat{\rho}_i} = \frac{\theta_{i+1} - \theta_{i-1}}{2\Delta \hat{\rho}}, \quad \frac{\partial^2 \theta}{\partial \hat{\rho}^2} \Big|_{\hat{\rho}=\hat{\rho}_i} = \frac{\theta_{i+1} - 2\theta_i + \theta_{i-1}}{\Delta \hat{\rho}^2}. \qquad (26)$$

3.2. Model linearization

The discretized form of the PDE system (17)–(21) for the poloidal magnetic flux gradient and the ODE (22) for the plasma total energy yield a set of nonlinear ODEs of the form

$$\dot{Z} = f(Z, u), \qquad (27)$$

where

$$Z = [\theta_2, \theta_3, \dots, \theta_{n-1}, W]^T, \qquad (28)$$

$$u = [I_p, P_1, P_2, \dots, P_{n_{nbi}}]^T. \qquad (29)$$

Linearizing (27) is required for the design of the LQI. Thus, a first order Taylor approximation around a reference trajectory is given by

$$\dot{Z} = f(Z^{ref}, u^{ref}) + \frac{\partial f}{\partial Z} \Big|_{Z^{ref}, u^{ref}} (Z - Z^{ref}) + \frac{\partial f}{\partial u} \Big|_{Z^{ref}, u^{ref}} (u - u^{ref}), \qquad (30)$$

where the reference trajectory state Z^{ref} and input u^{ref} satisfies

$$\dot{Z}^{ref} = f(Z^{ref}, u^{ref}). \qquad (31)$$

By defining $\Delta Z = Z - Z^{ref}$, and $\Delta u = u - u^{ref}$, (30) becomes

$$\Delta \dot{Z} = A\Delta Z + B\Delta u, \tag{32}$$

$$A \triangleq \left.\frac{\partial f}{\partial Z}\right|_{Z^{ref}, u^{ref}}, \quad B \triangleq \left.\frac{\partial f}{\partial u}\right|_{Z^{ref}, u^{ref}}. \tag{33}$$

3.3. LQI control problem formulation

As the control objective is to track a desired output trajectory, namely the safety factor and the normalized beta, the state equation (32) needs to be complemented with an output equation. Therefore, using a Taylor series expansion around the reference trajectory and neglecting higher-order terms, the deviation of the safety factor is written as

$$\Delta q = \underbrace{\left.\frac{B_{\phi,0}\rho_b^2 \hat{\rho}}{\theta^2}\right|_{Z^{ref}, u^{ref}}}_{C_1} \Delta \theta, \tag{34}$$

where $\Delta q = q - q^{ref}$ and $\Delta \theta = \theta - \theta^{ref}$. The deviation of the normalized beta from its reference trajectory value is expressed as

$$\Delta \beta_N = \underbrace{\left.\frac{(2/3)/V_p}{B_{\phi,0}^2/(2\mu_0)}\frac{aB_{\phi,0}}{I_p}\right|_{Z^{ref}, u^{ref}}}_{C_2}\Delta W + \underbrace{\left.\frac{-(2/3)W/V_p}{B_{\phi,0}^2/(2\mu_0)}\frac{aB_{\phi,0}}{I_p^2}\right|_{Z^{ref}, u^{ref}}}_{D_2}\Delta u, \tag{35}$$

where $\Delta \beta_N = \beta_N - \beta_N^{ref}$ and $\Delta W = W - W^{ref}$. The output equation takes the form

$$\Delta y = C\Delta Z + D\Delta u, \tag{36}$$

where

$$\Delta y = y - y^{ref} = [\Delta q, \Delta \beta_N]^T, \quad C = \begin{bmatrix} C_1 & 0_1 \\ 0_2 & C_2 \end{bmatrix}, \quad D = \begin{bmatrix} 0_3 \\ D_2 \end{bmatrix}, \tag{37}$$

and where $0_1 \in \mathbb{R}^{(1)\times(1)}$, $0_2 \in \mathbb{R}^{(1)\times(n-2)}$, $0_3 \in \mathbb{R}^{(1)\times(m)}$, and m is the number of control inputs.

Suppose that Z^{tar} and u^{tar} are the target states and inputs, respectively, that satisfy the governing equation

$$\dot{Z}^{tar} = f(Z^{tar}, u^{tar}). \tag{38}$$

Linearizing the above equation around a reference trajectory Z^{ref}, u^{ref} results in linear equations of the form

$$\Delta \dot{Z}^d = A\Delta Z^d + B\Delta u^d, \tag{39}$$

$$\Delta y^d = C\Delta Z^d + D\Delta u^d, \tag{40}$$

where $\Delta Z^d = Z^{tar} - Z^{ref}$, $\Delta y^d = y^{tar} - y^{ref}$, and $\Delta u^d = u^{tar} - u^{ref}$. Subtracting (39) and (40) from (32) and (36), respectively, results in the following error model

$$\Delta \dot{\bar{Z}} = A\Delta \bar{Z} + B\Delta \bar{u}, \tag{41}$$

$$\Delta \bar{y} = C\Delta \bar{Z} + D\Delta \bar{u} \tag{42}$$

with $\Delta \bar{Z} = \Delta Z - \Delta Z^d$, $\Delta \bar{y} = \Delta y - \Delta y^d$, and $\Delta \bar{u} = \Delta u - \Delta u^d$. To eliminate any steady state error, the error state $\Delta \bar{Z}$ is augmented with the time integral of the output error $\Delta \bar{y}$

$$e(t) = \int_{t_0}^{t} \Delta \bar{y}(\tau)d\tau = \int_{t_0}^{t}(y - y^{tar})(\tau)d\tau. \tag{43}$$

Thus, the new augmented state-space system is given by

$$\dot{\bar{x}} = \bar{A}(t)\bar{x}(t) + \bar{B}(t)\Delta \bar{u}(t), \tag{44}$$

$$\bar{x} \triangleq \begin{bmatrix} e(t) \\ \Delta \bar{Z}(t) \end{bmatrix}, \quad \bar{A} \triangleq \begin{bmatrix} 0 & C \\ 0 & A \end{bmatrix}, \quad \bar{B} \triangleq \begin{bmatrix} D \\ B \end{bmatrix}. \tag{45}$$

With the incorporation of the integral error as a state in the control model, the linear–quadratic regulator becomes a linear–quadratic integral controller. The LQI optimal control problem can be stated as

$$\min_{\Delta \bar{u}} J(t_0) = \bar{x}^T(t_f)P(t_f)\bar{x}(t_f) + \int_{t_0}^{t_f}(\bar{x}^T Q\bar{x} + \Delta \bar{u}^T R\Delta \bar{u})dt, \tag{46}$$

subject to $Q \in \mathbb{R}^{(m+n)\times(m+n)}, \quad R \in \mathbb{R}^{m\times m}. \tag{47}$

The solution of the LQI problem formulated in (46) and (47) is obtained by solving the differential Riccati equation

$$\dot{P} = -P\bar{A} - \bar{A}^T P + P\bar{B}R^{-1}\bar{B}^T P - Q, \tag{48}$$

using $P(t_f)$ from (46), where P is a symmetric positive definite matrix used to compute the feedback gain K needed for the feedback input $\Delta \bar{u}$,

$$K = R^{-1}\bar{B}^T P, \tag{49}$$

$$\Delta \bar{u} = -K\bar{x}. \tag{50}$$

During the flattop phase of the discharge, the augmented matrices $\bar{A}$ and $\bar{B}$ remain approximately time-invariant. In this case, the matrix P can be approximated by $\bar{P}$, which is obtained by solving the algebraic Riccati equation,

$$\bar{A}^T \bar{P} + \bar{P}\bar{A} - \bar{P}\bar{B}R^{-1}\bar{B}^T \bar{P} + Q = 0. \tag{51}$$

This steady-state solution of the LQI problem (46)–(47) assumes that $\lim_{t\to\infty} P = \bar{P}$, i.e. the sequence $P(t)$ converges to a constant matrix $\bar{P}$. In this case, the integral in (46) is formally defined between 0 and ∞. The overall control architecture is shown in Fig. 3.

4. Controller testing in COTSIM for an NSTX-U scenario

4.1. Implemented plasma models in COTSIM

The LQI controller presented in Section 3 has been tested using COTSIM, which is a control-oriented 1D simulator developed by the Plasma Control Group at Lehigh University. The simulation study in this work combines the MDE with the electron heat transport equation, which can be written as

$$\frac{3}{2}\frac{\partial}{\partial t}[n_e T_e] = \frac{1}{\rho_b^2 \hat{H}}\frac{1}{\hat{\rho}}\frac{\partial}{\partial \hat{\rho}}\left[\hat{\rho}\frac{\hat{G}\hat{H}^2}{\hat{F}}\left(\chi_e n_e \frac{\partial T_e}{\partial \hat{\rho}}\right)\right] + Q_e, \tag{52}$$

where χ_e is the electron thermal diffusivity, and Q_e is the electron-heat deposition from different sources such as Ohmic, radiation, and electron–ion collision heating. Different analytical models are available in COTSIM for neoclassical and anomalous transport such as Chang-Hinton, Bohm/gyro-Bohm model, and Coppi–Tang.

4.2. Simulation study in NSTX-U scenario

The ability of the controller to regulate the q profile as well as β_N around desired targets for NSTX-U scenarios has been studied in simulations. The feedforward inputs are held constant at 1 MA for the plasma current and 1 MW for each of the NBI powers. The plasma current and all 6 NBIs are used as actuators for this study. The constraints of the physical actuators are held at different levels: 0.3–1.5 MA for the plasma current, and 0.0–3.0 MW for each of the NBI powers. The controlled variables are $q(\hat{\rho} = 0.1, 0.3, 0.5, 0.7, 0.9)$, and β_N. The feedback controller is activated at 2 sec.

The targets used in the feedforward (FF) + feedback (FB) case have been generated in a separate simulation run by varying the evolutions of NBI powers and plasma current. This guarantees that the targets are indeed feasible. Fig. 4(a) shows the q profile at $t = 4$ s, while Fig. 4(b)–(e) show its evolution at $\hat{\rho} = 0.1, 0.5, 0.7, 0.9$. The evolution of β_N is shown in Fig. 4(f). The figures compare FF and FF+FB evolutions, showing how the FB controller "corrects" the FF evolution in order to avoid the deviations from the targets starting at around $t = 2.5$ s. This correction of the plasma trajectory is achieved by modifying the FF
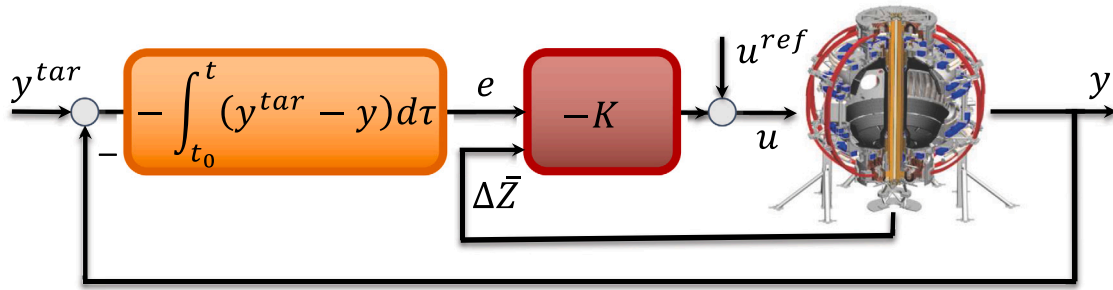
Fig. 3. Architecture of the LQI scheme, where the control component $\Delta\bar{u}$ is obtained as a state-feedback law based on the augmented state $\bar{x} = [e^T \ \Delta\bar{Z}^T]^T$.
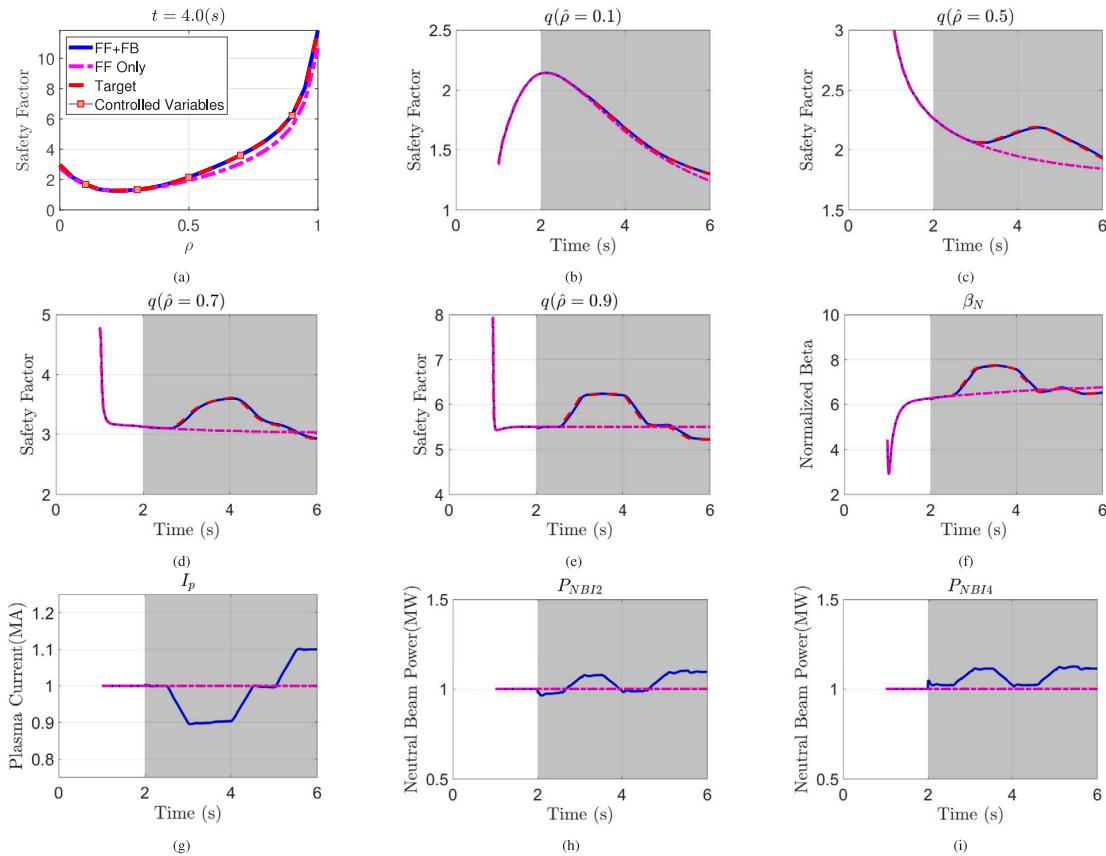

Fig. 4. Nonlinear simulations using the Coppi–Tang model comparing the time evolutions of the feedforward-only and feedforward + feedback solutions with the targets: (a) safety factor profile at $t = 4$ s.; (b) time evolution of the safety factor profile at $\hat{\rho} = 0.1$; (c) time evolution of the safety factor profile at $\hat{\rho} = 0.5$; (d) time evolution of the safety factor profile at $\hat{\rho} = 0.7$; (e) time evolution of the safety factor profile at $\hat{\rho} = 0.9$; (f) time evolution of the normalized beta; (g) time evolution of the plasma current; (h) time evolution of the second NBI power; (i) time evolution of the fourth NBI power.

control inputs as shown in Fig. 4(g)–(i). The LQI controller shows not only good performance in tracking the q-profile and β_N targets but also robustness since the simulations are carried out using nonlinear models with a complexity much higher than those used for control synthesis.

5. Conclusion

In this work, an optimal control algorithm has been proposed to tackle the problem of simultaneously controlling the safety-factor profile and normalized beta in NSTX-U. Linear control-oriented models that govern the evolutions of the poloidal magnetic gradient and the plasma total energy have been developed and used to synthesize an LQI controller. The LQI controller has been tested in higher-fidelity nonlinear simulations that show the capability by the controller of robustly regulating the safety factor profile and the normalized beta

in NSTX-U. Possible future work includes augmenting the controller to regulate additional plasma parameters such as internal inductance. Moreover, the controller will be tested in experiments to further assess its capability and robustness.

Declaration of competing interest

The authors declare that they have no known competing financial interests or personal relationships that could have appeared to influence the work reported in this paper.

Data availability

The authors do not have permission to share data.

Acknowledgments

References

[1] S. Gerhardt, R. Andre, J. Menard, Exploration of the equilibrium operating space for NSTX-upgrade, Nucl. Fusion 52 (8) (2012) 083020.

[2] F.L. Hinton, R.D. Hazeltine, Theory of plasma transport in toroidal confinement systems, Rev. Modern Phys. 48 (2) (1976) 239–308.

[3] W. Shi, W. Wehner, J. Barton, M. Boyer, E. Schuster, D. Moreau, M. Walker, J. Ferron, T. Luce, D. Humphreys, B. Penaflor, R. Johnson, Data-driven robust control of the plasma rotational transform profile and normalized beta dynamics for advanced tokamak scenarios in DIII-D, Fusion Eng. Des. 117 (2017) 39–57.

[4] A. Pajares, E. Schuster, Nonlinear robust safety factor profile control in tokamaks via feedback linearization and nonlinear damping techniques, in: 2018 IEEE Conference on Control Technology and Applications, CCTA, 2018, pp. 306–311, http://dx.doi.org/10.1109/CCTA.2018.8511450.

[5] J.E. Barton, M.D. Boyer, W. Shi, E. Schuster, T.C. Luce, J.R. Ferron, M.L. Walker, D.A. Humphreys, B.G. Penaflor, R.D. Johnson, Toroidal current profile control during low confinement mode plasma discharges in DIII-D via first-principles-driven model-based robust control synthesis, Nucl. Fusion 52 (12) (2012) 123018.

[6] W. Shi, W. Wehner, J. Barton, M.D. Boyer, E. Schuster, D. Moreau, T.C. Luce, J.R. Ferron, M.L. Walker, D.A. Humphreys, B.G. Penaflor, R.D. Johnson, Multivariable robust control of the plasma rotational transform profile for advanced tokamak scenarios in DIII-D, in: 2012 American Control Conference, ACC, 2012, pp. 5037–5042.

[7] S.T. Paruchuri, A. Pajares, E. Schuster, Minimum safety factor control in tokamaks via optimal allocation of spatially moving electron cyclotron current drive, in: 2021 60th IEEE Conference on Decision and Control, CDC, 2021, pp. 454–459, http://dx.doi.org/10.1109/CDC45484.2021.9683130.

[8] F.B. Argomedo, E. Witrant, C. Prieur, S. Brémond, R. Nouailletas, J.-F. Artaud, Lyapunov-based distributed control of the safety-factor profile in a tokamak plasma, Nucl. Fusion 53 (3) (2013) 033005.

[9] Y.V. Mitrishkin, V.A. Ivanov, Combined nonlinear tokamak plasma current profile control system design and simulation with input constraints, IFAC Proc. Vol. 44 (1) (2011) 3728–3733, 18th IFAC World Congress.

[10] Z.O. Ilhan, M.D. Boyer, E. Schuster, TRANSP-based closed-loop simulations of current profile optimal regulation in NSTX-upgrade, Fusion Eng. Des. 146 (2019) 555–558, SI:SOFT-30.

[11] Z.O. Ilhan, W. Wehner, J. Barton, E. Schuster, D. Gates, S. Gerhardt, J. Menard, First-principles-driven model-based optimal control of the current profile in NSTX-U, in: 2015 IEEE Conference on Control Applications, CCA, 2015, pp. 1303–1308, http://dx.doi.org/10.1109/CCA.2015.7320792.

[12] E. Maljaars, F. Felici, M. de Baar, J. van Dongen, G. Hogeweij, P. Geelen, M. Steinbuch, Control of the tokamak safety factor profile with time-varying constraints using MPC, Nucl. Fusion 55 (2) (2015) 023001.

[13] Z.O. Ilhan, W.P. Wehner, E. Schuster, Model predictive control with integral action for the rotational transform profile tracking in NSTX-U, in: 2016 IEEE Conference on Control Applications, CCA, 2016, pp. 623–628, http://dx.doi.org/10.1109/CCA.2016.7587899.

[14] I. Garrido, A.J. Garrido, S. Coda, H.B. Le, J.M. Moret, Real time hybrid model predictive control for the current profile of the Tokamak à configuration variable TCV, Energies 9 (8) (2016).

[15] S. Wang, E. Witrant, D. Moreau, Robust control of q-profile and β_n using data-driven models on EAST, Fusion Eng. Des. 162 (2021) 112071.

[16] Z. Wang, H. Wang, E. Schuster, Z. Luo, Y. Huang, Q. Yuan, B. Xiao, D. Humphreys, Optimal shaping of the safety factor profile in the EAST tokamak, in: 2021 IEEE Conference on Control Technology and Applications, CCTA, 2021, pp. 63–68, http://dx.doi.org/10.1109/CCTA48906.2021.9658937.

[17] H. Wang, W.P. Wehner, E. Schuster, Combined current profile and plasma energy control via model predictive control in the EAST tokamak, in: 2018 26th Mediterranean Conference on Control and Automation, MED, 2018, pp. 1–9, http://dx.doi.org/10.1109/MED.2018.8442553.

[18] A. Pajares, E. Schuster, Current profile and normalized beta control via feedback linearization and Lyapunov techniques, Nucl. Fusion 61 (3) (2021) 036006.

[19] W. Shi, W. Wehner, J. Barton, M.D. Boyer, E. Schuster, A. Kritz, D. Moreau, T.C. Luce, J.R. Ferron, M.L. Walker, D.A. Humphreys, B.G. Penaflor, R. Johnson, PTRANSP simulation and experimental test of a robust current profile and β_N controller for off-axis current drive scenarios in the DIII-D tokamak, in: 2013 American Control Conference, 2013, pp. 1225–1230, http://dx.doi.org/10.1109/ACC.2013.6580003.

[20] J.E. Barton, K. Besseghir, J. Lister, E. Schuster, Physics-based control-oriented modeling and robust feedback control of the plasma safety factor profile and stored energy dynamics in ITER, Plasma Phys. Control. Fusion 57 (11) (2015) 115003.

[21] M. Boyer, R. Andre, D. Gates, S. Gerhardt, I. Goumiri, J. Menard, Central safety factor and β_N control on NSTX-U via beam power and plasma boundary shape modification, using TRANSP for closed loop simulations, Nucl. Fusion 55 (5) (2015) 053033.

[22] J. Wesson, D.J. Campbell, Tokamaks, Oxford University Press, 2018.

[23] Y. Ou, T. Luce, E. Schuster, J. Ferron, M. Walker, C. Xu, D. Humphreys, Towards model-based current profile control at DIII-D, Fusion Eng. Des. 82 (5) (2007) 1153–1160, Proceedings of the 24th Symposium on Fusion Technology.

[24] O. Sauter, C. Angioni, Y.R. Lin-Liu, Neoclassical conductivity and bootstrap current formulas for general axisymmetric equilibria and arbitrary collisionality regime, Phys. Plasmas 6 (7) (1999) 2834–2839.

[25] ITER Physics Expert Group on Confinement and Transport and ITER Physics Expert Group on Confinement Modelling and Database and ITER Physics Basis Editors, Chapter 2: Plasma confinement and transport, Nucl. Fusion 39 (12) (1999) 2175.